https://doi.org/10.3311/PPme.37831

Periodica Polytechnica Mechanical Engineering, 69(2), pp. 93–102, 2025

Development of a New Method for Characterize Resistance to Cyclic Tensile Load in Mono and Hybrid Composites

Mihály László Vas[1], Tibor Czigány[1,2], Péter Tamás-Bényei[1,2,3*]

[1] Department of Polymer Engineering, Faculty of Mechanical Engineering, Budapest University of Technology and Economics, H-1111 Budapest, Műegyetem rkp. 3., Hungary
[2] HUN-REN-BME Research Group for Composite Science and Technology, H-1111 Budapest, Műegyetem rkp. 3., Hungary
[3] MTA-BME Lendület Sustainable Polymers Research Group, Budapest, H-1111, Műegyetem rkp. 3., Hungary
[*] Corresponding author, e-mail: tamasp@pt.bme.hu

Received: 05 September 2024, Accepted: 22 May 2025, Published online: 30 May 2025

Abstract

The objective of our study was to investigate and describe the durability of mono and hybrid composite materials reinforced with various fabrics (namely, glass, carbon, and basalt) and an epoxy resin matrix against repetitive loads, with a particular focus on their potential use in wind turbine blades. The mechanical properties of these materials were evaluated through repeated tensile tests involving high deflection and low cycle numbers. A new approach was introduced for characterizing and comparing the performance of glass, carbon, and basalt fiber reinforced epoxy composites. Our results led to the development of a novel model to evaluate a new mechanical property, the asymptotic modulus, which can be used to assess the resistance of composite materials to multi-cycle tensile loads in a faster and simpler manner. Differences between the measured and by our model predicted values were low, the values of determination coefficient were higher than 94%.

Keywords

hybrid composite, epoxy resin, cyclic load

1 Introduction

In the last decade fibre reinforced composites became widely used materials thanks to their beneficial properties (special structure, low weight, high performance, tailored anisotropy) [1, 2]. Due to the international energetical situation the renewable energy forms receives higher interest. 2023 the installed global renewable capacity was about 4000 GW. From the renewables the wind energy is the most promising and dynamically growing (with 27% compared to 2020) renewable energy form [3, 4]. The tree highest renewable type was the hydropower (1411.3 GW), solar energy (1552.3 GW) and the wind energy (1007.2 GW) [5]. Wind turbines blades are made from polymer composites materials with application of different synthetic fibres. Due to the high and long-term loads and stresses [6, 7] and the weather conditions [8, 9] the structure of the wind turbine blades were built up from fibreglass or carbon fibre with thermoset matrix generally. In the field of engineering application commonly used reinforcements are glass and carbon fabrics but nowadays basalt fabric receives higher consideration as well [10–12]. Basalt is a volcanic rock which can be found around the world. Basalt fibres are made of molten rock by a similar method as producing fibreglass. Basalt fibre and its composites (mono and hybrid reinforcements with thermoplastic and thermoset matrix as well) could be bioinert, "green" engineering materials [13–15]. The chemical composition and the mechanical properties of basalt fibres are similar to the glass fibres [16]. Thanks to their beneficial properties basalt fibre reinforced thermosets are frequently investigated research areas and basalt composites are suitable as the raw materials of wind turbine blades [17, 18]. Sarasini et al. [19, 20] investigated the effect of basalt fibre hybridization on the impact of behavior of epoxy resin. Residual strength of composites with different stacking sequences (basalt, glass) was examined. During the tests, acoustic signals were monitored by an acoustic emission device. According to their results, the basalt-skin/glass-core type performed a little better than the intercalated type. Pure basalt fibre reinforced composites performed better compared to glass and hybrid fibre reinforced materials. Lim et al. [21] investigated mechanical

Cite this article as: Vas, M. L., Czigány, T., Tamás-Bényei, P. "Development of a New Method for Characterize Resistance to Cyclic Tensile Load in Mono and Hybrid Composites", Periodica Polytechnica Mechanical Engineering, 69(2), pp. 93–102, 2025. https://doi.org/10.3311/PPme.37831

properties of carbon/basalt epoxy hybrid composites built up of basalt skin with carbon core (BSCC) and carbon skin with basalt core (CSBC). On the basis of their results, flexural strength and modulus of CSBC were 32% and 245% higher than those of BSCC, respectively. Fracture toughness of CSBC was 10% lower than that of BSCC. Sun et al. [22] analyzed the mechanical properties of hybrid composites reinforced by carbon and basalt fibres. Seven symmetric composite laminates with different hybrid ratios and stacking sequences were fabricated by the vacuum assisted resin transfer molding. Their results showed the failure resistance of pure carbon fibre composites was improved after inserting basalt fibre layers.

According to the investigation of mechanical properties of basalt fibre reinforced epoxy composites, it can be declared these materials are ideal engineering materials. In some cases, the load of engineering materials was not only static or dynamic but cyclic. The load of applied polymer composites was various but typically cyclic as well as fatiguing [23]. Mechanical properties become worse with increasing cycle number. Usually, the number of cycles which caused failure could be more than a million, but it depended on the frequency as well as the load [24]. Four main damage modes have been observed: matrix cracking, delamination, fibre-matrix debonding, and fibre fracture [25, 26]. Matrix cracking and delamination arise early the lifetime, while other damages initiate at the beginning of lifetime and grow until critical failure.

The determination of the fatigue limit of composite materials has traditionally relied on the "Wohler curve" or "S-N" curve [27]. Nevertheless, constructing an S-N curve necessitates numerous prolonged tests under various stress levels [28], making the process both costly and time-consuming [29]. Therefore, there is a significant need for innovative approaches that can expedite the determination of a material's fatigue limit and overcome these limitations. Subramanian et al. [30] created a model to describe the influence of the fibre-matrix interface on tensile fatigue behavior. Using this model can be specified how the constituent materials should be put together to improve fatigue performance. Revuelta et al. [31] used Weibull distribution model fatigue response of polymer composites and proved complex fatigue models could not better fit the measured conventional fatigue curves than linear models. Jia et al. [32] developed a new fatigue limit determination method based on the thermographic data. Different stress levels were selected for the experiments, with each trial concluding either at the point of specimen failure or after achieving a maximum of 106 cycles without failure. The analysis of the results obtained from various methods indicated that their approach can be effectively utilized to determine the fatigue limit of composite laminates. Zhao et al. [33] analyzed behavior and damage mechanism of basalt fiber reinforced polymers. The static and fatigue properties of different resin matrixes based on BFRP composites were experimentally investigated with static and fatigue tests combined with in-situ SEM observation. Zhao et al. [34] investigated fatigue behavior and failure mechanism of basalt FRP composites under long-term cyclic loads in normal environmental conditions. The specimens were under long-term cyclic loads up to 107 cycles. Their results revealed that under the high level of stress, the critical fibre breaking failure is the dominant damage, while the matrix cracking and interfacial debonding are main damage patterns at the low and middle fatigue stress level for BFRP. Wang et al. [35] studied fatigue degradation and life prediction of basalt fibre reinforced polymer composites after saltwater corrosion. The results show that the static strength of the BFRP shows negligible degradation after ageing in the salt solution, whereas the detrimental effect of saltwater becomes apparent under fatigue loading. The fatigue life prediction indicates that the fatigue strength of BFRP degrades to an acceptable level after the occurrence of saltwater corrosion. Various models were created to describe mechanical behavior and residual strength [36–40] of reinforced composites moreover to predict the lifetime [41–44]. The drawback of these methods usually is that they require a large number of measurements to be taken, and the process is slow.

Due to the wide-range application of carbon, glass and basalt fibre composite we aimed the analysis of these materials. The aim of our paper was to create a model by a novelty approach to describe the mechanical behavior and to characterize the asymptotic material property (a tensile modulus) of glass, basalt, and carbon fabric reinforced mono and hybrid composites subjected to cyclic tensile load faster and simpler as the common methods.

2 Theoretical background

In Section 2, we introduce the theoretical background of our research and the development process of our mathematical model.

2.1 Cyclic load and the viscoelastic response

When quasi-static multi-cycle tensile tests are executed using symmetric triangle wave deformation stimulus $X(t)$,

the absolute values of the rates of loading and unloading are the same $\left(\dot{X}_0\right)$ and constant where t_0 is the half period time and X_0 is the maximum deformation (Eq. (1)) (Fig. 1):

$$X_0 = \dot{X}_0 t_0. \tag{1}$$

The stimulus in the n^{th} (n = 1, 2, …) cycle is (Eq. (2)):

$$X_n(t) = \begin{cases} \dot{X}_0 t - 2(n-1)X_0, & (2n-2)t_0 \le t < (2n-1)t_0 \\ 2nX_0 - \dot{X}_0 t, & (2n-1)t_0 \le t < 2nt_0 \end{cases}, \tag{2}$$

and the whole stimulus process is the sum of the oscillation cycles (Eq. (3)):

$$X(t) = \sum_{n=1}^{\infty} X_n(t). \tag{3}$$

The derivative of the stimulus process is a square signal sequence with an alternating sign (Fig. 1) the value of which in the nth cycle (n = 1, 2, …) is given by (Eq. (4)):

$$\dot{X}_n(t) = \begin{cases} \dot{X}_0, & (2n-2)t_0 \le t < (2n-1)t_0 \\ -\dot{X}_0, & (2n-1)t_0 \le t < 2nt_0 \end{cases}. \tag{4}$$

Sum of the previous cycles is the whole derivate progress (Eq. (5)):

$$\dot{X}(t) = \sum_{n=1}^{\infty} \dot{X}_n(t) = \sum_{n=1}^{\infty} \left[d_{2n-1}(t,t_0) - d_{2n}(t,t_0) \right], \tag{5}$$

where the window function $d_k(t, t_0)$ (k = 1, 2, …) is a difference (Eq. (6)):

$$d_k(t,t_0) = 1\left(t - (k-1)t_0\right) - 1\left(t - kt_0\right), \tag{6}$$

and $1(t)$ is the so-called unit jump or Heaviside function (Eq. (7)):

$$1(t) = \begin{cases} 0, & t \le 0 \\ 1, & 0 < t \end{cases}. \tag{7}$$

When the behavior of specimens is linear viscoelastic and the relaxation modulus function ($E(t)$) is known hence, on the basis of Boltzmann-superposition principle, the stress as an answer ($Y = \sigma(t)$) to the deformation stimulus ($X = \varepsilon(t)$) can be given by convolution integral [39] (Eq. (8)):

$$\sigma(t) = \int_0^t E(t-u)\dot{\varepsilon}(u)\,du. \tag{8}$$

In addition, if we examine half-cycles and t comes within the k^{th} half-cycle ($(k-1)t_0 <= t < kt_0$) then according to Eq. (5) – taking into considering the alternating signs – the two half-cycle could be handled in the same way and the stress answer in the k^{th} cycle is as follows (Eq. (9)):

$$\sigma_k(t) = \dot{\varepsilon}_0 \sum_{i=1}^{k} (-1)^{i-1} d_k(t,t_0) \int_{(i-1)t_0}^{t} E(t-u)\,du, \tag{9}$$

where we assumed that integration and summarization can be exchanged.

2.2 Modelling of cyclic tensile test results using generalized Standard-Solid model

Investigated materials were fibre reinforced (fibreglass, basalt fibre, carbon fibre) epoxy composites where remaining deformation is negligible compared to instantaneous and retarded elastic deformation therefore supposable, results of cyclic tensile and bending test with cyclic deformation could be described by a simple or a generalized Standard Solid linear viscoelastic material model consisting of a spring and a single or multi-element Maxwell model (Fig. 2). Due to the parallel connection every branch of the model receives the same deformation stimulus hence the resulting force or stress is the sum of those in the branches therefore each branch could be investigated separately.

Required number of Maxwell branches (N) is determined by the accuracy of the description. In order to obtain a suitable model firstly the behavior of a single Maxwell branch then the generalized Standard-Solid model subjected to the cyclic deformation load in Fig. 1 are considered.

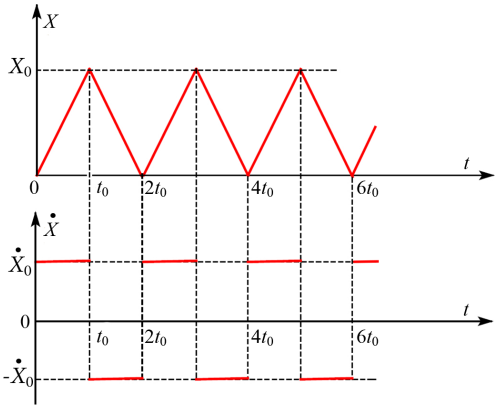

Fig. 1 Cyclic deformation stimulus and its derivative

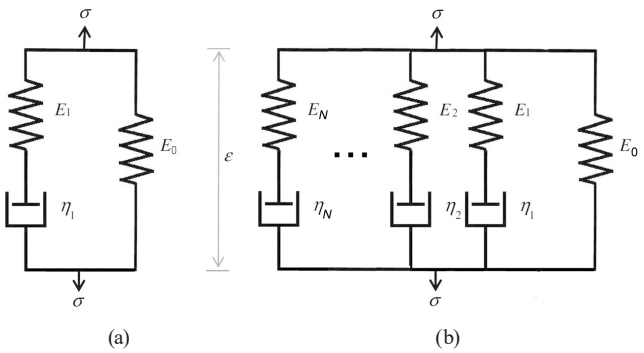

Fig. 2 (a) Standard-Solid model and (b) its generalized form

2.2.1 Application of a simple Standard-Solid model

Spring and viscose elements of Maxwell model are assumed to follow the Hooke's law and the Newton's law respectively. Due to the previous facts, the two parameters of model are elastic modulus (E) and dynamic viscosity factor (η) (Fig. 2) [29]. The differential equation of Maxwell model describes the relationship between strain ($X = \varepsilon$) as stimulus and engineering stress ($Y = \sigma$) as answer. Equation (10) shows the Bode format of differential equation of Maxwell model [29]:

$$\tau\dot{\sigma} + \sigma = E\tau\dot{\varepsilon}, \tag{10}$$

where dot above variables means the time derivative and t is the time constant of the model (Eq. (11)):

$$\tau = \eta / E. \tag{11}$$

When $X = e$ deformation stimulus starts at $t = 0$ then in k^{th} half-cycle the $Y = s$ stress-answer is given by general solution (Eq. (12)) of 1st order inhomogeneous differential Eq. (10) [29]:

$$\sigma_k(t) = \sigma_{k-1}\left((k-1)t_0\right)e^{-\frac{t-(k-1)t_0}{\tau}} + E\int_{(k-1)t_0}^{t}\dot{\varepsilon}(u)e^{-\frac{t-u}{\tau}}du,$$

$$(k-1)t_0 \le t \le kt_0,\ \ k = 1,2,\ldots, \tag{12}$$

where according to Fig. 1 and Eq. (4) the derivative of the strain is in case of $(k-1)\ t_0 \le t \le kt_0$ (Eq. (13)):

$$\dot{\varepsilon}(t) = \begin{cases} \dot{\varepsilon}_0 = \varepsilon_0 / t_0, k \text{ odd} \\ -\dot{\varepsilon}_0 = -\varepsilon_0 / t_0, k \text{ even} \end{cases}. \tag{13}$$

Based on Eq. (12) and using the initial condition, $\sigma(0) = 0$, a compact form of stress values at the end of the k^{th} half-cycle ($k = 1, 2, \ldots$) could be obtained (Eq. (14)):

$$\sigma_k(kt_0) = (-1)^{k-1}\sigma_1(t_0)\frac{1-(-1)^k e^{-\frac{kt_0}{\tau}}}{1+e^{-\frac{t_0}{\tau}}} = (-1)^{k-1}E\varepsilon_0\frac{1-e^{-\frac{t_0}{\tau}}}{\frac{t_0}{\tau}}\frac{1-(-1)^k e^{-\frac{kt_0}{\tau}}}{1+e^{-\frac{t_0}{\tau}}}. \tag{14}$$

With increasing cycle number the stress at the end of half-cycle tends to a finite value, which is positive at positive peaks while negative at negative peaks (Eq. (15)):

$$\sigma_k(kt_0) \underset{k\to\infty}{\to} \frac{\sigma_1(t_0)}{1+e^{-\frac{t_0}{\tau}}} \times \begin{cases} +1, \ k \text{ odd} \\ -1, \ k \text{ even} \end{cases}. \tag{15}$$

According to the previous equations the positive and negative peaks are separable. Monotone decreasing positive stress peaks will be obtained at odd k values ($k = 2n-1$, $n = 1, 2, \ldots$) tending to a finite value if $n \to \infty$ (Eq. (16)):

$$\sigma_{2n-1}\left((2n-1)t_0\right) = \sigma_1(t_0)\frac{1+e^{-\frac{(2n-1)t_0}{\tau}}}{1+e^{-\frac{t_0}{\tau}}} = E\varepsilon_0\frac{1-e^{-\frac{t_0}{\tau}}}{\frac{t_0}{\tau}}\frac{1+e^{-\frac{(2n-1)t_0}{\tau}}}{1+e^{-\frac{t_0}{\tau}}} \underset{n\to\infty}{\to} E\varepsilon_0\frac{1-e^{-\frac{t_0}{\tau}}}{\frac{t_0}{\tau}\left(1+e^{-\frac{t_0}{\tau}}\right)}. \tag{16}$$

For demonstration Fig. 3 shows the change of stress peaks by cyclic deformation stimulus according to the Eq. (16) at chosen model data.

In Fig. 3 the peak values by Eq. (16) are normalized by the first stress peak value, $E\varepsilon_0$ (setting data: $L_0 = 100$ mm, $\Delta L = 5$ mm, $v = 10$ mm/min $\to \varepsilon_0 = 0.05$, $\dot{\varepsilon}_0 \approx 0.0017$/s, $t_0 \approx 30$ s; chosen data: $E = 1000$ MPa, $\eta = 10000$ MPa $\to \tau = 50$ s, $t_0/\tau \approx 0.6$). Rate of decreasing is determined by the exponential terms and t_0/τ ratio. The positive stress peaks are monotone decreasing and after some peaks the decreasing is very low, and the sequence is considerable steady.

2.2.2 Generalized Standard-Solid model and the asymptotic modulus

In the case of generalized Standard-Solid model (Fig. 2 (b)) the resultant stress is the sum of those rising in the model branches (Eq. (17)):

$$\sigma(t) = \sigma_0(t) + \sigma_1(t) + \sigma_2(t) + \ldots + \sigma_N(t), \tag{17}$$

where $\sigma_1(t)$, …, $\sigma_N(t)$ are the stresses in the Maxwell branches analyzed above, while $\sigma_0(t)$ is the stress in the

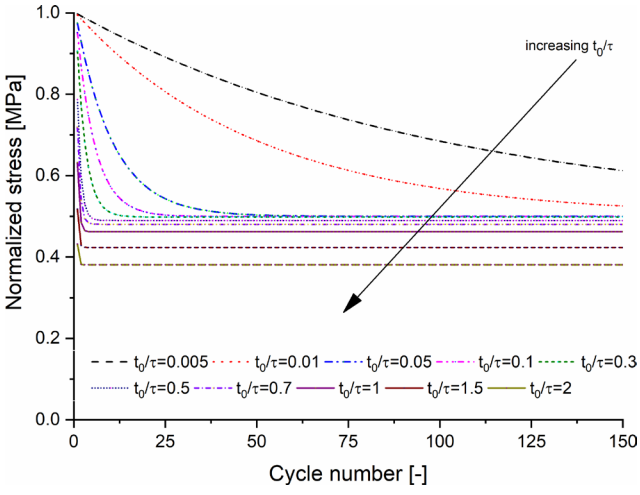

Fig. 3 Change of normalized Maxwell stress peaks as a function of cycle number at different value of ratio t_0/τ

spring branch that is proportional to the deformation stimulus (Eq. (18)):

$$\sigma_0(t) = E_0 \varepsilon(t). \tag{18}$$

In every branch positive stress peak arises in moments of positive deformation peaks, therefore the resulting positive stress peaks are given by the sum of branch-peaks. It is equal in the $k^{\text{th}} = (2n-1)^{\text{th}}$ half-cycle the left-hand side of Eqs. (19) and (20) while the right-hand sides of them give the asymptotic positive stress peak values when $n \to \infty$:

$$\begin{aligned}&\sigma_{2n-1}\left((2n-1)t_0\right)\\&= E_0\varepsilon_0 + \sum_{k=1}^{N} E_k \varepsilon_0 g_{2n-1}\left(\frac{t_{0_k}}{\tau_k}\right)\\&\underset{n\to\infty}{\to} E_0\varepsilon_0 + \sum_{k=1}^{N} E_k \varepsilon_0 g_{\infty}\left(\frac{t_{0_k}}{\tau_k}\right) = \sigma_{\infty},\end{aligned} \tag{19}$$

where:

$$\begin{aligned}&g_{2n-1}\left(\frac{t_{0_k}}{\tau_k}\right)\\&= \frac{1-e^{-\frac{t_{0_k}}{\tau_k}}}{\frac{t_{ok}}{\tau_k}} \frac{1+e^{-\frac{(2n-1)t_{0_k}}{\tau_k}}}{1+e^{-\frac{t_{0_k}}{\tau_k}}} \underset{n\to\infty}{\to} \frac{1-e^{-\frac{t_{0_k}}{\tau_k}}}{\frac{t_{0_k}}{\tau_k}} \frac{1}{1+e^{-\frac{t_{0_k}}{\tau_k}}}\\&= g_{\infty}\left(\frac{t_{0_k}}{\tau_k}\right).\end{aligned} \tag{20}$$

Stress peaks arise at the end of a t_0 wide interval where the value of deformation is ε_0. A kind of chord modulus could be obtained by dividing the stress peaks by ε_0. The asymptotic value of this ratio, E_∞, is the so-called asymptotic cyclic modulus that characterizes the asymptotic specific resistance of the given material against of cyclic deformation thus it can be considered an important quality property of materials (Eq. (21)):

$$E_{\infty} = E_0 + \sum_{k=1}^{N} E_k g_{\infty}\left(\frac{t_{0_k}}{\tau_k}\right). \tag{21}$$

3 Materials and methods

Ipox MR 3010 epoxy laminating resin was used (Ipox chemicals GmbH, Germany) with MH3124 curing agent (Ipox chemicals GmbH, Germany) as matrix material. The mixing weight ratio was 100:33. Glass (Saint-Gobain Vetrotex, Germany), basalt (Basaltex, Belgium), and carbon fabrics (SGL Group, Germany) of a surface density of 220 g/m^2 and plain-woven structure were used as reinforcements with silane sizing. Composite sheets with 2 mm average thickness have been prepared by hand layup process at room temperature. Every sheet was built up of 6 layers and alternating layer order was used in case of hybrid structures (Table 1).

The fibre content was 50 ± 2 wt% in every case. Specimens were cured in a Heraeus UT20 drying oven at 80 °C for 2 h after molding. After post-curing process specimens were cut with a Mutronic Diadisc 4200 cutting machine. Tensile tests were carried out according to EN ISO 527-4:1997 [45] by a Zwick Z020 universal testing machine with 10 mm/min crosshead speed at room temperature. The gauge length was 100 mm. In every case strength decrease was investigated at high displacement (in every cycle repeated from 0% until 80% of break elongation) by performing 150 cycles.

4 Results and discussion

Tensile stress peaks as the results of multi-cycle tensile tests are shown in Fig. 4. According to our results with increasing cycle number strength of mono and hybrid composites decreased strictly monotonic. Strength decrease was caused by damage of fibre-matrix interfacial adhesion

Table 1 Layer structures of investigated mono and hybrid composites

Designation	Number of layers		
	Glass fabric	Basalt fabric	Carbon fabric
GFEP	6	0	0
BFEP	0	6	0
CFEP	0	0	6
GFCFEP	3	0	3
BFCFEP	0	3	3

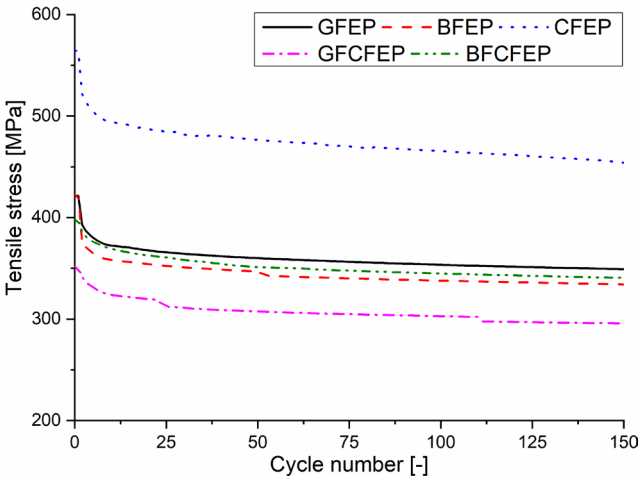

Fig. 4 Results of multi-cycle tensile test

and of matrices moreover of mono filaments. In case of mono composites basalt fabric reinforced composites had the highest tensile stress decrease (21%) while it was 20% for the carbon fabric and 17% for the glass fabric, however in case of basalt-carbon fabrics reinforced hybrid composites the decrease was 14% meanwhile for glass-carbon fabric reinforced it was 16%. Lower decrease of hybrid composites was possibly caused by the synergetic effect between carbon and basalt fabrics. A mathematical model could be created based on our results and based on linear viscoelastic (LVE) behavior discussed above an asymptotic material property could be defined and calculated.

4.1 Measured and modelled stress peaks and the asymptotic modulus

Fig. 4 shows the variation of stress peaks measured during cyclic tensile tests carried out on different composite materials. In most cases at the beginning the peak values decrease steeply but after a few cycles the steepness of decreasing is lower. In Fig. 5 the tendency of measured stress peak values normalized by initial values can be seen. Based on results it can be concluded that disregarding the initial part of curves the decreasing of normalized stress peaks are similar to each other, they are following parallel trends therefore similar model could be used for every investigated material.

According to the measurements stress peaks could be described by a generalized Standard-Solid model with two Maxwell branches (Fig. 2 (b)).

On the basis of Eq. (17) the resultant stress is the sum of the branch stresses (Eq. (22)):

$$\sigma(t)=\sigma_0(t)+\sigma_1(t)+\sigma_2(t). \tag{22}$$

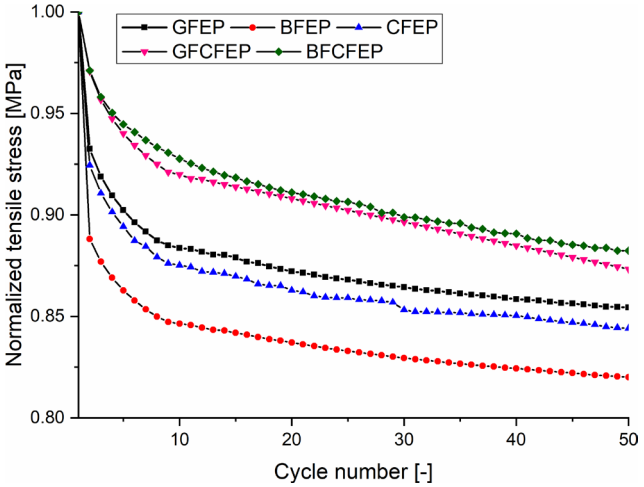

Fig. 5 Normalized measured tensile stress peaks vs. cycle number

Accordingly, the asymptotic tensile modulus (Eq. (23)) qualifying the investigated composite materials can be obtained by Eq. (19):

$$E_\infty = E_0 + E_1 g_\infty\left(t_{0_1}/\tau_1\right) + E_2 g_\infty\left(t_{0_2}/\tau_2\right). \tag{23}$$

Comparison of positive stress peaks obtained by measurements and by modelling is shown in Fig. 6.

Good quality of fitting is characterized by the mean squared errors lower than 0.65% and by the values of determination coefficient higher than 94%. Obtained model parameters are summarized by Tables 2 and 3. Based on obtained model parameters the calculated asymptotic modulus values are summarized by Fig. 7.

According to the results, among the mono composites carbon fabric reinforced epoxy resist better against cyclic load than the others as basalt-carbon fabric reinforced composite does among hybrid materials. Due to the positive hybrid effect between basalt-carbon and between glass-carbon fabrics asymptotic modulus was 11% and 6% higher than calculated by hybrid rule of mixture, respectively. Based on the asymptotic modulus materials can be qualified and compared.

5 Conclusions

This paper investigates the mechanical behavior of mono and hybrid composites reinforced with glass, basalt, and carbon fabrics, subjected to cyclic tensile loads. The results show that carbon fabric-reinforced composites exhibit the best resistance to cyclic loads, with a calculated tensile stress value of 454 MPa, while epoxy resin reinforced with glass-carbon fabric has the lowest resistance at 296 MPa.

Based on these findings, a mathematical model was developed to estimate a new material property, the asymptotic tensile modulus, which effectively characterizes the asymptotic resistance of mono and hybrid composites reinforced with glass, basalt, and carbon fabrics against cyclic loads. Our method offers faster and much easier estimation for residual modulus as the previous methods. Our model demonstrated good quality of fitting, with a relative mean squared error below 0.65% and a determination coefficient above 94%. The asymptotic modulus results indicate that carbon fabric-reinforced epoxy exhibits the best resistance to cyclic loads (8458 MPa) among the investigated materials, and the basalt-carbon fabric reinforced composite (8215 MPa) shows the highest resistance among the hybrid materials.

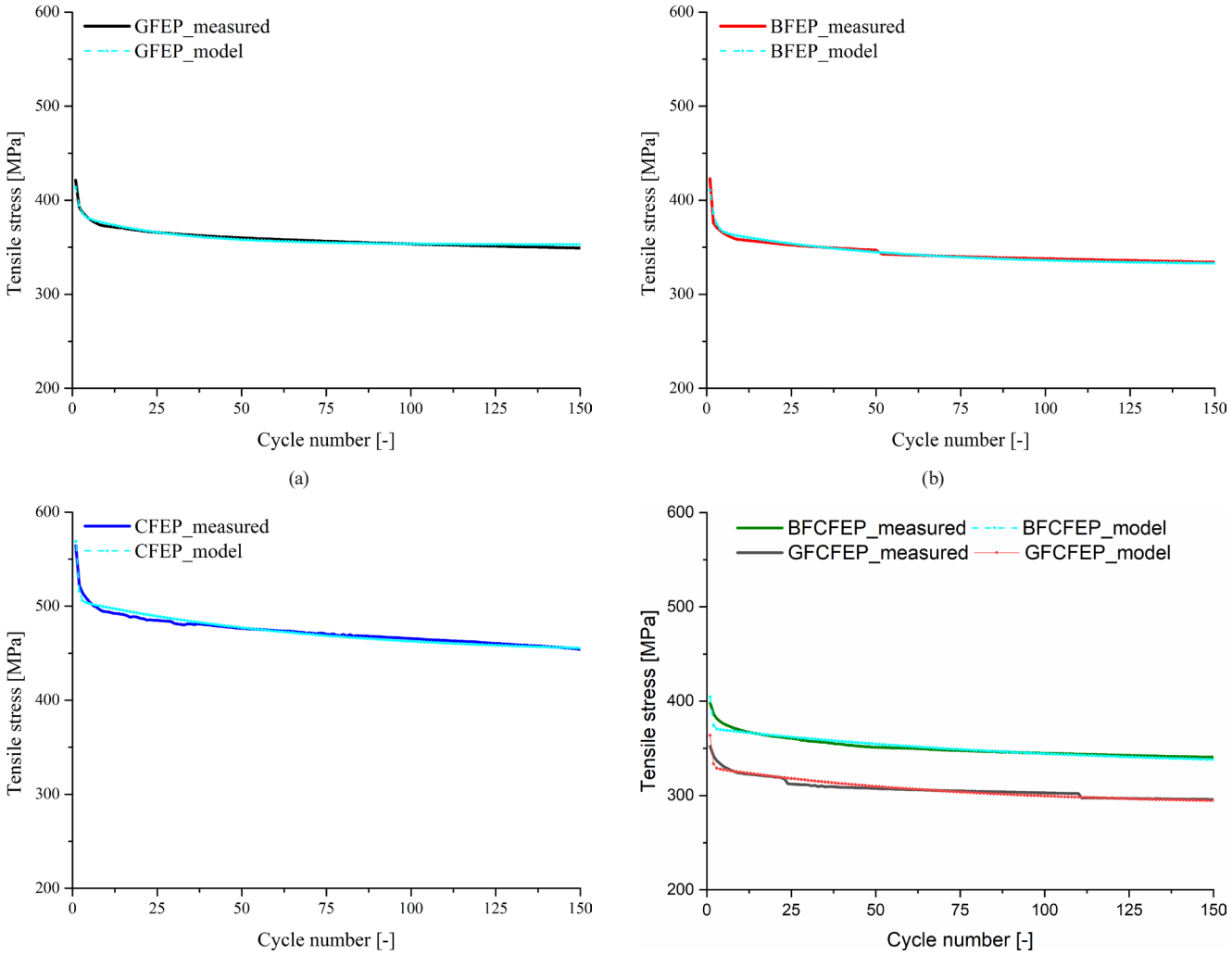

Fig. 6 Results of modelling positive stress peaks of epoxy resin composites reinforced by: (a) glass fibre (GFEP), (b) basalt fibre (BFEP), (c) carbon fibre (CFEP), (d) glass-carbon fibre (GFCFEP) and basalt-carbon fibre (BFCFEP)

Table 2 Model parameters of mono composites tested with cyclic tensile load

Model parameters		Materials		
		GFEP	BFEP	CFEP
E_0	MPa	1412	1403	2180
E_1	MPa	922	2473	6050
E_2	MPa	3957	4324	4520
η_1	MPa	0.124	4.462	9.903
η_2	MPa	2.121	0.192	0.221
$(t_0/\tau)_1$	–	0.470	0.010	0.007
$(t_0/\tau)_2$	–	0.018	0.410	0.870

Table 3 Model parameters of hybrid composites tested with cyclic tensile load

Model parameters		Materials	
		GFCFEP	BFCFEP
E_0	MPa	2010	2133
E_1	MPa	5050	5671
E_2	MPa	3900	4576
η_1	MPa	6.891	10.238
η_2	MPa	0.121	0.122
$(t_0/\tau)_1$	–	0.007	0.005
$(t_0/\tau)_2$	–	1.000	1.120

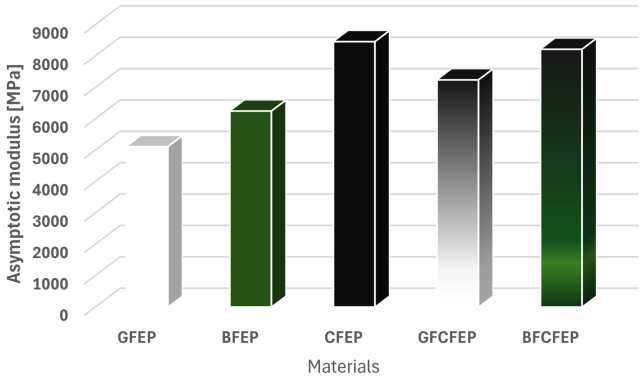

Fig. 7 Asymptotic modulus of materials tested with cyclic tensile load

Acknowledgement

The research reported in this paper is part of project no. BME-NVA-02, implemented with the support provided by the Ministry of Innovation and Technology of Hungary from the National Research, Development and Innovation Fund, financed under the TKP2021 funding scheme. This research was also supported by the ÚNKP-23-5-BME-309 New National Excellence Program of The Ministry for Culture and Innovation from the source of the National Research, Development and Innovation Fund. This project was supported by the János Bolyai Research Scholarship of the Hungarian Academy of Sciences (BO/00658/21/6).

References

[1] Petrény, R., Bezerédi, Á., Mészáros, L. "Electrically conductive polymer composites: Today's most versatile materials?", Express Polymer Letters, 18(7), pp. 673–674, 2024. https://doi.org/10.3144/expresspolymlett.2024.49

[2] Szebényi, G. "High-performance composites and medical applications of polymers – the sunny sides of the polymer industry", Express Polymer Letters, 16(11), 1113, 2022. https://doi.org/10.3144/expresspolymlett.2022.81

[3] International Renewable Energy Agency (IRENA) "Renewable capacity statistics 2024", International Renewable Energy Agency (IRENA), 2024. ISBN 978-92-9260-587-2 [online] Available at: https://www.irena.org/Publications/2024/Mar/Renewable-capacity-statistics-2024 [Accessed: 24 June 2024]

[4] Kong, K., Dyer, K., Payne, C., Hamerton, I., Weaver, P. M. "Progress and Trends in Damage Detection Methods, Maintenance, and Data-driven Monitoring of Wind Turbine Blades – A Review", Renewable Energy Focus, 44, pp. 390–412, 2023. https://doi.org/10.1016/j.ref.2022.08.005

[5] International Energy Agency (IEA) "Renewables 2023: Analysis and forecast to 2028", International Energy Agency (IEA), Paris, France, 2023. [online] Available at: https://www.iea.org/reports/renewables-2023 [Accessed: 24 June 2024]

[6] Rahman, A. S. "Design of cost-effective and efficient fiber-reinforced composite blades for wind turbines", Reinforced Plastics, 63(1), pp. 21–25, 2019. https://doi.org/10.1016/j.repl.2017.11.010

[7] O'Leary, K., Pakrashi, V., Kelliher, D. "Optimization of composite material tower for offshore wind turbine structures", Renewable Energy, 140, pp. 928–942, 2019. https://doi.org/10.1016/j.renene.2019.03.101

[8] Zhang, M., Li, X., Tong, J., Xu, J. "Load control of floating wind turbine on a Tension-Leg-Platform subject to extreme wind condition", Renewable Energy, 151, pp. 993–1007, 2020. https://doi.org/10.1016/j.renene.2019.11.093

[9] Wei, X., Ng, B. F., Zhao, X. "Aeroelastic load control of large and flexible wind turbines through mechanically driven flaps", Journal of the Franklin Institute, 356(14), pp. 7810–7835, 2019. https://doi.org/10.1016/j.jfranklin.2019.02.030

[10] Monaldo, E., Nerilli, F., Vairo, G. "Basalt-based fiber-reinforced materials and structural applications in civil engineering", Composite Structures, 214, pp. 246–263, 2019. https://doi.org/10.1016/j.compstruct.2019.02.002

[11] Adole, O., Barekar, N., Anguilano, L., Minton, T., Novytskyi, A., McKay, B. "Fibre/matrix intermetallic phase formation in novel aluminium-basalt composites", Materials Letters, 239, pp. 128–131, 2019. https://doi.org/10.1016/j.matlet.2018.12.079

[12] Elmahdy, A., Verleysen, P. "Mechanical behavior of basalt and glass textile composites at high strain rates: A comparison", Polymer Testing, 81, 106224, 2020. https://doi.org/10.1016/j.polymertesting.2019.106224

[13] Tábi, T., Égerházi, A. Z., Tamás, P., Czigány, T., Kovács, J. G. "Investigation of injection moulded poly(lactic acid) reinforced with long basalt fibres", Composites Part A: Applied Science and Manufacturing, 64, pp. 99–106, 2014. https://doi.org/10.1016/j.compositesa.2014.05.001

[14] Tábi, T., Tamás, P., Kovács, J. G. "Chopped basalt fibres: A new perspective in reinforcing poly(lactic acid) to produce injection moulded engineering composites from renewable and natural resources", eXPRESS Polymer Letters, 7(2), pp. 107–119, 2013. https://doi.org/10.3144/expresspolymlett.2013.11

[15] Yu, S., Hwang, Y. H., Hwang, J. Y., Hong, S. H. "Analytical study on the 3D-printed structure and mechanical properties of basalt fiber-reinforced PLA composites using X-ray microscopy", Composites Science and Technology, 175, pp. 18–27, 2019. https://doi.org/10.1016/j.compscitech.2019.03.005

[16] Deák, T., Czigány, T. "Chemical Composition and Mechanical Properties of Basalt and Glass Fibers: A Comparison", Textile Research Journal, 79(7), pp. 645–651, 2009. https://doi.org/10.1177/0040517508095597

[17] Dhand, V., Mittal, G., Rhee, K. Y., Park, S.-J., Hui, D. "A short review on basalt fiber reinforced polymer composites", Composites Part B: Engineering, 73, pp. 166–180, 2015. https://doi.org/10.1016/j.compositesb.2014.12.011

[18] Fiore, V., Di Bella, G., Valenza, A. "Glass–basalt/epoxy hybrid composites for marine applications", Materials & Design, 32(4), pp. 2091–2099, 2011.
https://doi.org/10.1016/j.matdes.2010.11.043

[19] Sarasini, F., Tirillò, J., Valente, M., Valenete, T., Cioffi, S., Iannace, S., Sorrentino, L. "Effect of basalt fiber hybridization on the impact behaviour under low impact velocity of glass/basalt woven fabric/epoxy resin composites", Composites Part A: Applied Science and Manufacturing, 47, pp. 109–123, 2013.
https://doi.org/10.1016/j.compositesa.2012.11.021

[20] Sarasini, F., Tirillò, J., Valente, M., Ferrante, L., Cioffi, S., Iannace, S., Sorrentino, L. "Hybrid composites based on aramid and basalt woven fabrics: Impact damage modes and residual flexural properties", Materials & Design, 49, pp. 290–302, 2013.
https://doi.org/10.1016/j.matdes.2013.01.010

[21] Lim, J. I., Rhee, K. Y., Kim, H. J., Jung, D. H. "Effect of stacking sequence on the flexural and fracture properties of carbon/basalt/epoxy hybrid composites", Carbon Letters, 15(2), pp. 125–128, 2014.
https://doi.org/10.5714/CL.2014.15.2.125

[22] Sun, G., Tong, S., Chen, D., Gong, Z., Li, Q. "Mechanical properties of hybrid composites reinforced by carbon and basalt fibers", International Journal of Mechanical Sciences, 148, pp. 636–651, 2018.
https://doi.org/10.1016/j.ijmecsci.2018.08.007

[23] Mortazavian, S., Fatemi, A. "Fatigue behavior and modeling of short fiber reinforced polymer composites: A literature review", International Journal of Fatigue, 70, pp. 297–321, 2015.
https://doi.org/10.1016/j.ijfatigue.2014.10.005

[24] Halpin, J. C., Jerina, K. L., Johnson, T. A. "Characterization of Composites for the Purpose of Reliability Evaluation", In: Whitney, J. M. (ed.) Analysis of the Test Methods for High Modulus Fibers and Composites, ASTM International, 1973, pp. 5–64. ISBN 978-0-8031-0701-4
https://doi.org/10.1520/STP36479S

[25] Reifsnider, K. L., Henneke, E. G., Stinchcomb, W. W., Duke, J. C. "Damage mechanics and NDE of composite laminates", In: Hashin, Z., Herakovich, C. T. (eds.) Mechanics of Composite Materials: Recent Advances, Pergamon, 1983, pp. 399–420. ISBN 978-0-08-029384-4
https://doi.org/10.1016/C2013-0-03667-5

[26] Razvan, A., Reifsnider, K. L. "Fiber fracture and strength degradation in unidirectional graphite/epoxy composite materials", Theoretical and Applied Fracture Mechanics, 16(1), pp. 81–89, 1991.
https://doi.org/10.1016/0167-8442(91)90043-J

[27] Pascual, F. G., Meeker, W. Q. "Estimating Fatigue Curves With the Random Fatigue-Limit Model", Technometrics, 41(4), pp. 277–289, 1999.
https://doi.org/10.1080/00401706.1999.10485925

[28] Feng, Y., Gao, C., He, Y., An, T., Fan, C., Zhang, H. "Investigation on tension–tension fatigue performances and reliability fatigue life of T700/MTM46 composite laminates", Composite Structures, 136, pp. 64–74, 2016.
https://doi.org/10.1016/j.compstruct.2015.09.057

[29] Harris, B. "Fatigue in Composites: Science and Technology of the Fatigue Response of Fibre-Reinforced Plastics", Woodhead Publishing, 2003. ISBN 978-1-85573-608-5

[30] Subramanian, S., Reifsnider, K. L., Stinchcomb, W. W. "A cumulative damage model to predict the fatigue life of composite laminates including the effect of a fibre-matrix interphase", International Journal of Fatigue, 17(5), pp. 343–351, 1995.
https://doi.org/10.1016/0142-1123(95)99735-S

[31] Revuelta, D., Cuartero, J., Miravete, A., Clemente, R. "A new approach to fatigue analysis in composites based on residual strength degradation", Composite Structures, 48(1–3), pp. 183–186, 2000.
https://doi.org/10.1016/S0263-8223(99)00093-8

[32] Jia, Z., Pastor, M.-L., Garnier, C., Gong, X. "A new method for determination of fatigue limit of composite laminates based on thermographic data", International Journal of Fatigue, 168, 107445, 2023.
https://doi.org/10.1016/j.ijfatigue.2022.107445

[33] Zhao, X., Wang, X., Wu, Z., Wu, J. "Experimental study on effect of resin matrix in basalt fiber reinforced polymer composites under static and fatigue loading", Construction and Building Materials, 242, 118121, 2020.
https://doi.org/10.1016/j.conbuildmat.2020.118121

[34] Zhao, X., Wang, X., Wu, Z., Zhu, Z. "Fatigue behavior and failure mechanism of basalt FRP composites under long-term cyclic loads", International Journal of Fatigue, 88, pp. 58–67, 2016.
https://doi.org/10.1016/j.ijfatigue.2016.03.004

[35] Wang, X., Zhao, X., Wu, Z. "Fatigue degradation and life prediction of basalt fiber-reinforced polymer composites after saltwater corrosion", Materials & Design, 163, 107529, 2019.
https://doi.org/10.1016/j.matdes.2018.12.001

[36] Broutman, L. J., Sahu, S. "A New Theory to Predict Cumulative Fatigue Damage in Fiberglass Reinforced Plastics", In: Corten, H. T. (ed.) Composite Materials: Testing and Design, ASTM International, 1972, pp. 170–188. ISBN 978-0-8031-0134-0
https://doi.org/10.1520/STP27746S

[37] Hahn, H. T., Kim, R. Y. "Proof Testing of Composite Materials", Journal of Composite Materials, 9(3), pp. 297–311, 1975.
https://doi.org/10.1177/002199837500900308

[38] Yang, J. N., Liu, M. D. "Residual Strength Degradation Model and Theory of Periodic Proof Tests for Graphite/Epoxy Laminates", Journal of Composite Materials, 11(2), pp. 176–203, 1977.
https://doi.org/10.1177/002199837701100205

[39] Chou, P. C., Croman, R. "Residual Strength in Fatigue Based on the Strength-Life Equal Rank Assumption", Journal of Composite Materials, 12(2), pp. 177–194, 1978.
https://doi.org/10.1177/002199837801200206

[40] Adam, T., Dickson, R. F., Jones, C. J., Reiter, H., Harris, B. "A Power Law Fatigue Damage Model for Fibre-Reinforced Plastic Laminates", Proceedings of the Institution of Mechanical Engineers, Part C: Journal of Mechanical Engineering Science, 200(3), pp. 155–166, 1986.
https://doi.org/10.1243/PIME_PROC_1986_200_111_02

[41] Song, D.-Y., Otani, N. "Fatigue life prediction of cross-ply composite laminates", Materials Science and Engineering: A, 238(2), pp. 329–335, 1997.
https://doi.org/10.1016/S0921-5093(97)00427-9

[42] D'Amore, A., Giorgio, M., Grassia, L. "Modeling the residual strength of carbon fiber reinforced composites subjected to cyclic loading", International Journal of Fatigue, 78, pp. 31–37, 2015.
https://doi.org/10.1016/j.ijfatigue.2015.03.012

[43] Gonabadi, H., Oila, A., Yadav, A., Bull, S. "Fatigue life prediction of composite tidal turbine blades", Ocean Engineering, 260, 111903, 2022.
https://doi.org/10.1016/j.oceaneng.2022.111903

[44] Vas, L. M., Kling, S., Czigány, T., Czél, G. "New method for determining the bending modulus of solid and hollow fibers from deflection tests", Textile Research Journal, 87(5), pp. 542–551, 2016.
https://doi.org/10.1177/0040517516632476

[45] CEN "EN ISO 527-4:1997 Plastics - Determination of tensile properties - Part 4: Test conditions for isotropic and orthotopic fibre-reinforced plastic composites (ISO 527-4:1997)", European Committee for Standardization, Brussels, Belgium, 1997.